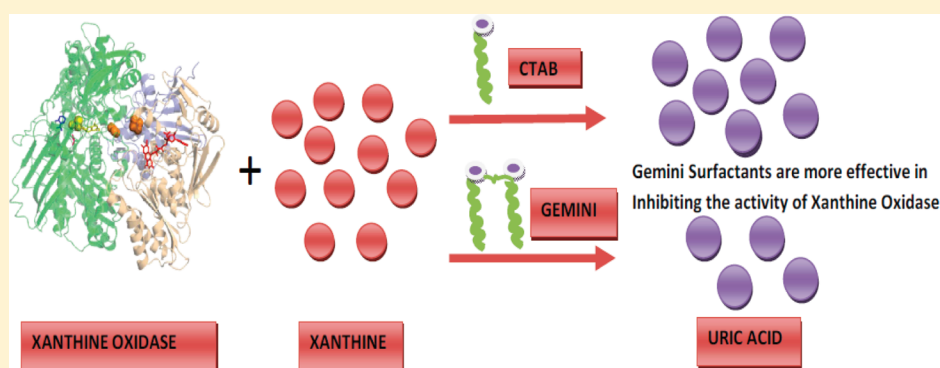


Interaction of Cetyltrimethylammonium Bromide and Its Gemini Homologue Bis(cetyldimethylammonium)butane Dibromide with Xanthine Oxidase

Mohammad Amin Mir,^{†,§} Javed Masood Khan,[‡] Rizwan Hasan Khan,[‡] Aijaz Ahmad Dar,^{*,†} and Ghulam Mohammad Rather^{*,†}

[†]Department of Chemistry, University of Kashmir, Srinagar 190006, J&K, India

[‡]Interdisciplinary Biotechnology Unit, Aligarh Muslim University, Aligarh 202002, India



ABSTRACT: The interaction of xanthine oxidase (XO), a key enzyme in purine metabolism, with cetyltrimethylammonium bromide (CTAB) and bis(cetyldimethylammonium)butane dibromide ($C_{16}C_4C_{16}Br_2$) has been studied using tensiometry, spectrofluorometry, spectrophotometry, and circular dichroism at pH 7.4 and 25 °C. The tensiometric profiles of CTAB and $C_{16}C_4C_{16}Br_2$ in the presence of XO exhibit a single break at a lower surfactant concentration termed as C_1 compared to their CMC in the buffered solution and show the existence of interaction between the surfactants and the enzyme. The results of the multitechnique approach showed that, although both CTAB as well as $C_{16}C_4C_{16}Br_2$ interact with the XO, $C_{16}C_4C_{16}Br_2$ interacts more strongly than its conventional single chain counterpart. Fluorescence and absorption measurements revealed that, compared to CTAB, $C_{16}C_4C_{16}Br_2$ is more effective in unfolding the enzyme. Change in XO activity by the surfactants was in concurrence with the structural alterations monitored by circular dichroism and showed structural stabilization of XO at higher surfactant concentrations, consistent with the aggregation results. This stabilization has been explained in light of strong tendency of $C_{16}C_4C_{16}Br_2$ for micellar growth and membrane/water stabilization of proteins by membrane-like fragments provided by higher concentrations of $C_{16}C_4C_{16}Br_2$. The results are related to the stronger electrostatic and hydrophobic forces in $C_{16}C_4C_{16}Br_2$, owing to the presence of two charged headgroups and two hydrophobic tails.

INTRODUCTION

The interaction of proteins with surfactants has received a great deal of interest for many years due to its application in a variety of industrial, biological, cosmetic, pharmaceutical, and food processing systems.^{1–4} The binding of surfactants with proteins is usually determined by the surfactant features. It is known in general that, compared to anionic surfactants, cationic surfactants interact weakly with the proteins as a consequence of smaller relevance of electrostatic interactions at the pHs of interest.⁵ However, the shapes of binding isotherms of these two kinds of surfactants with the same protein have been found to be similar^{5,6} and are well studied.⁷ Initially, at low surfactant concentrations, ionic surfactants bind noncooperatively to the oppositely charged high energy sites of proteins thereby unfolding the protein. As the surfactant concentration is increased, the binding becomes cooperative, and ultimately, the protein is saturated by the surfactant and its aggregates.²

Xanthine oxidase (XO), a complex molybdoflavo protein, is a key enzyme in purine metabolism that has attracted lots of attention because of its potential role in tissue and vascular injuries, as well as in inflammatory diseases and chronic heart failure.^{8,9} It catalyzes the oxidation of hypoxanthine to xanthine and that of xanthine to uric acid with concomitant reduction of molecular oxygen.¹⁰ This last step results in the production of superoxide anion and hydrogen peroxide, two reactive oxygen species that have been associated with the potential damaging role of the enzyme.^{9–11} The enzyme is a homodimer, each monomer is composed of an N-terminal domain containing two iron–sulfur centers (Fe/S I and Fe/S II), a central flavin adenine dinucleotide (FAD) domain, and a C-terminal

Received: August 14, 2011

Revised: April 23, 2012

Published: April 24, 2012

molybdopterin-binding domain with the four redox centers aligned in an almost linear fashion.^{12–14} Substrate oxidation occurs at the molybdenum site, which becomes reduced from Mo(VI) to Mo(IV) in the process.¹⁵ The catalytic cycle is completed by electron transfer from molybdenum to the $[\text{Fe}_2\text{--S}_2]$ clusters and then to the flavin, where the electrons are donated to an acceptor such as O_2 .^{12,13}

The production of reactive oxygen species by XO and its damaging consequences has prompted investigations into the ability of some compounds, such as allopurinol, nitric oxide, or macrocyclic copper II, to control and/or inhibit the enzyme activity, or scavenge the free radicals produced.^{8,16,17} A number of metallic and nonmetallic compounds have been reported^{18–21} to alter the activity of XO depending on the compound. However, important classes of amphiphilic molecules, surfactants, have not been tested so far to control the activity of XO. As mentioned above, because of their ability to bind and denature proteins, surfactants are expected to alter the activity of XO.

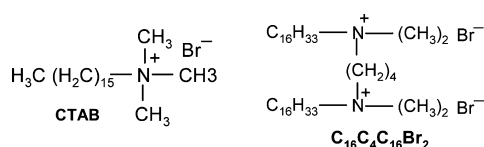
Cationic gemini surfactants, made up of two hydrophobic chains and two polar head groups covalently linked through a spacer group, have a number of unique aggregation properties^{22–25} in comparison to conventional single-chain surfactants. These include much lower critical micelle concentration (CMC), strong dependence on spacer structure, special aggregate morphology, strong hydrophobic microdomains, and so on. Because of their unique aggregation properties, the interaction of cationic gemini surfactants with proteins have revealed that such surfactants interact more efficiently with proteins as compared to conventional single chain surfactants.^{26–31}

In the present work, we report the effect of gemini surfactant $\text{C}_{16}\text{C}_4\text{C}_{16}\text{Br}_2$ on the activity of XO along with detailed investigation on structural changes of XO caused by its interaction with the surfactant. For comparison, parallel measurements have been made between XO and CTAB. Structural and activity alterations of XO were assessed by circular dichroism, intrinsic and extrinsic fluorescence, and electronic absorption studies.

EXPERIMENTAL SECTION

Materials. Bovine milk xanthine oxidase (XO, Sigma), cetyltrimethylammonium bromide (CTAB, Sigma), and 1-anilino-8-naphthalene sulfonic acid (ANS, Sigma) were used as received. The gemini bis(cetyldimethylammonium)butane dibromide ($\text{C}_{16}\text{H}_{33}(\text{CH}_3)_2\text{N}^+(\text{CH}_2)_4\text{N}^+(\text{CH}_3)_2\text{C}_{16}\text{H}_{33}\cdot 2\text{Br}^-$) was synthesized and characterized as described elsewhere.³² The structure of the surfactants is given in the Scheme 1. All the stock solutions of XO, CTAB, and $\text{C}_{16}\text{C}_4\text{C}_{16}\text{Br}_2$ were prepared in 60 mM phosphate buffer of pH 7.4 with triple distilled water and utilized to prepare the samples of desired concentrations. The concentration of the XO solution was determined by measuring its absorbance at 280 nm, using an extinction coefficient of $11.26 \text{ mM}^{-1} \text{ cm}^{-1}$,³³

Scheme 1



on a Hitachi U-1500 spectrophotometer and was kept constant ($2 \mu\text{M}$) throughout the study.

Methods. Tensiometry. Surface tension measurements were made with a Krüss 9 Tensiometer (Germany) by the Whilhemmy plate method. Ten milliliters of $2 \mu\text{M}$ XO solution in phosphate buffer was taken in the sample vessel, and the surfactant concentration was varied by adding the appropriate aliquots of concentrated surfactant solution using a Hamilton microsyringe so that no more than 1.0 mL of surfactant solution was added to the XO solution to keep the protein concentration practically constant, and readings were taken after thorough mixing and temperature equilibration. The temperature was maintained at $25 \pm 0.1^\circ\text{C}$ by circulating water from a HAAKE GH thermostat. The accuracy of measurements was within 0.1 dyn cm^{-1} . The plate used was washed with acetone followed by triple distilled water and finally dried over a flame after every measurement. This nullified the effect expected due to adsorption of protein on the plate.

Fluorescence Measurements. The fluorescence spectra were collected at 25°C with a 1 cm path length cell using a Hitachi spectrofluorometer (Model 2500) equipped with a PC. The excitation and emission slits were set at 5 nm. The reference sample consisting of the buffer and the detergent did not give any fluorescence signal. The solution was excited at 295 nm, and the emission spectra were recorded in the range of 300–400 nm.

For extrinsic fluorescence measurements in the ANS binding studies, the excitation was set at 380 nm, and the emission spectra were taken in the range of 400–600 nm.

For aggregation studies, Rayleigh's scattering measurements were performed by observing emission at 350 nm after excitation at the same wavelength.

Circular Dichroism. CD measurements were carried out with a Jasco spectropolarimeter (Model J-720) equipped with a microcomputer. The instrument was calibrated with D-10-camphorsulfonic acid. All the CD measurements were carried out at 25°C with a thermostatically controlled cell holder attached to a Neslab RTE-110 water bath with an accuracy of $\pm 0.1^\circ\text{C}$. Far-UV CD spectra were taken in a cell of 1 mm path length over the wavelength range of 200–250 nm. A reference sample containing buffer and the detergent was subtracted from the CD signal for all measurements. The high tension voltage for the spectra obtained was found to be less than 600 V. Spectra were collected with a scan speed of 20 nm/min and response time of 1 s. Each spectrum is the average of four scans.

Spectrophotometry. The absorbance spectra were collected at 25°C with a 1 cm path length cell using a Shimadzu spectrophotometer (Model UV-1650) equipped with a PC. The surfactant concentration was kept the same in both the reference and the measurement cells to eliminate the effect of surfactant on UV absorbance.

Inhibitory activity of XO was measured spectrophotometrically³⁴ by following the oxidation of xanthine to uric acid at 295 nm. The assay was performed in 60 mM phosphate buffer of pH 7.4. The assay mixtures containing $2 \mu\text{M}$ XO ($50 \mu\text{L}$ of $100 \mu\text{M}$ XO stock solution) and the desired amount of the detergent were incubated for 1 h at 25°C before the activity measurements. The reaction was initiated by adding $62.5 \mu\text{L}$ of 4 mM Xanthine solution (final concentration $100 \mu\text{M}$); the final volume of the reaction mixture was always 2.5 mL. XO inhibitory activity, expressed as percentage inhibition of XO, was calculated as $(1 - \Delta A/\Delta A_0) \times 100$, where ΔA and ΔA_0 were taken as the increase in the absorbance of uric acid after

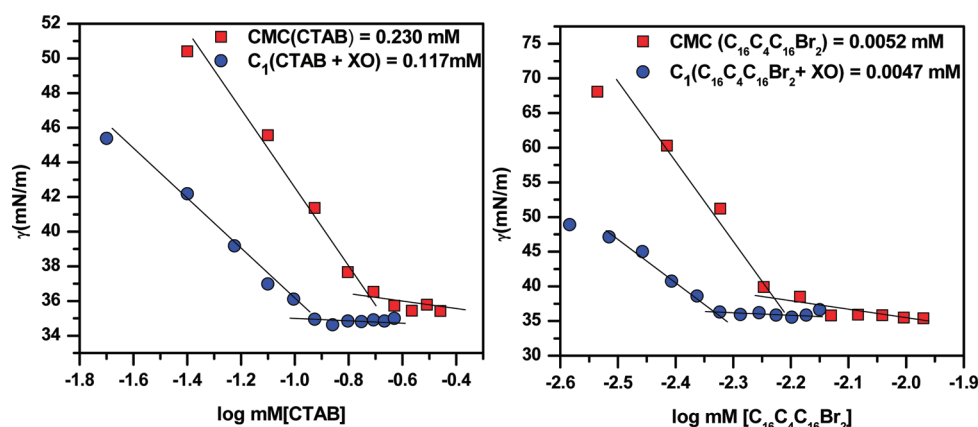


Figure 1. Tensiometric profiles in absence (squares) and presence of 2 μM XO (circles) for CTAB and $\text{C}_{16}\text{C}_4\text{C}_{16}\text{Br}_2$ at pH 7.4 and 25 $^{\circ}\text{C}$.

one minute with and without the surfactants, respectively. All the experiments were performed in triplicate.

RESULTS AND DISCUSSION

Surface Tension Measurements. The threshold concentration required for the self-aggregation of the surfactant, known as critical micelle concentration (CMC), can be taken from the break in the surface tension (γ) versus $\log[\text{surfactant}]$ profile.^{35–38} Above this concentration, the interfacial tension remains essentially constant reflecting that the surface concentration has reached a constant maximum value. Therefore, it is a general consensus that the interface gets saturated with the surfactant at CMC.³⁹ Tensiometric profiles for the addition of CTAB and $\text{C}_{16}\text{C}_4\text{C}_{16}\text{Br}_2$ to the buffer solution under identical experimental conditions are illustrated with squares in Figure 1. The CMCs of the CTAB and $\text{C}_{16}\text{C}_4\text{C}_{16}\text{Br}_2$ in buffer were lower compared to that in aqueous solution due to a decrease in the electrostatic repulsion between the charged head groups at elevated ionic strength.^{40,41}

Surface tension measurement is a simple and effective method of studying the interaction between macromolecules and surfactants. Deviation of tensiometric plots of surfactants in the presence of proteins from that of surfactants alone indicates the existence of interaction between the surfactant and the protein.⁴² The tensiometric profiles of CTAB and $\text{C}_{16}\text{C}_4\text{C}_{16}\text{Br}_2$ in the presence of XO are included in Figure 1 (circles) and show lower surface tension values than those in the absence of XO, due to the surface activity of XO ($\gamma = 55.3 \text{ mN/m}$ for 2 μM XO solution). The tensiometric profiles for CTAB and $\text{C}_{16}\text{C}_4\text{C}_{16}\text{Br}_2$ in the presence of XO exhibit a single break at a lower concentration (C_1) compared to their CMC values in the buffer solution. The interface in this regime is populated by surfactant monomers/surfactant–XO complexes. The interaction between proteins and ionic surfactants at the interface is dominated by the electrostatic interactions.^{43,44} Since the isoelectric point of XO is 5.3,⁴⁵ overall negative charge is expected on XO at pH 7.4. With an increase in concentration of CTAB and $\text{C}_{16}\text{C}_4\text{C}_{16}\text{Br}_2$, the available negative charges in the protein molecules are compensated by the oppositely charged surfactant ions, thus forming electroneutral complexes of enhanced surface activity compared to native protein. Because of the electrostatic attraction between the positively charged surfactant and negatively charged XO, the effective concentration of surfactant around XO is higher than that in bulk, so the C_1 is lower than the CMC in the XO free solutions. The

tensiometric results clearly indicate the existence of interaction between the surfactants and XO.

Aggregation Studies. The change in the scattering intensities at 350 nm of XO (FI_{350}) mainly arises from the change in number and/or size of complexes or adducts formed by the combination of XO and surfactant molecules.⁴⁶ The ability of these complexes or adducts to scatter light reflect their size/hydrodynamic radius, which is determined by the interaction of surfactants with XO. The surfactants that unfold the XO to a greater extent would effectively increase the hydrodynamic radius of resulting XO–surfactant complexes and hence FI_{350} . Figure 2 illustrates the change in FI_{350} with

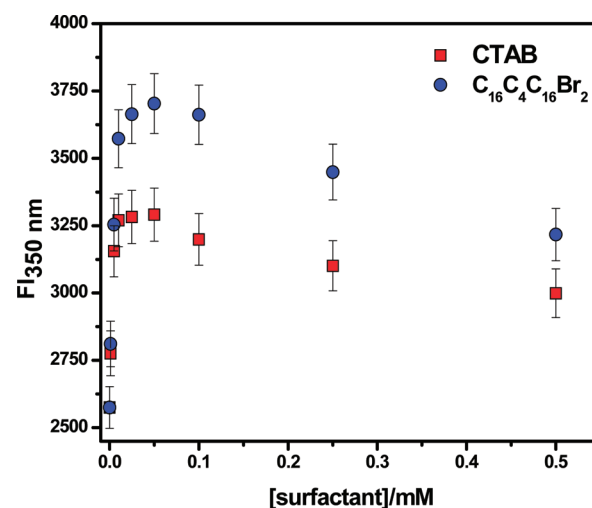


Figure 2. Variation of fluorescence intensity at 350 nm of 2 μM XO with the concentration of CTAB and $\text{C}_{16}\text{C}_4\text{C}_{16}\text{Br}_2$ at pH 7.4 and 25 $^{\circ}\text{C}$.

[surfactant] and indicates that the FI_{350} initially increases with increase in [surfactant] followed by a slight decrease particularly at higher concentrations. The FI_{350} increase being more pronounced in $\text{C}_{16}\text{C}_4\text{C}_{16}\text{Br}_2$ (1128 A.U.) than in CTAB (717 A.U.) is an indication of stronger interaction of the former with the XO, as suggested by earlier reports.^{26,28,31,47} The binding of surfactant to proteins and formation of protein–surfactant complexes are the consequences of electrostatic and hydrophobic interactions. The initial binding at a particular site facilitates the cooperative binding of other surfactant molecules through hydrophobic interactions,⁴⁸ leading to the formation of

micellar aggregates on the XO with increasing surfactant concentration. The electrostatic repulsion between these aggregates unfold the complexes thereby increasing their hydrodynamic radius and hence the FI_{350} . After attaining the maximum, the FI_{350} drops by 292 A.U. and 486 A.U. in presence of the CTAB and Gemini, respectively. The pronounced effect of the $C_{16}C_4C_{16}Br_2$ may be attributed to its hydrophobic spacer inducing lower solubility and hence stronger tendency to self-assemble around XO, two hydrophobic tails enhancing cooperative binding, higher charge density favoring electrostatic interactions, and architecture more suitable for micellar growth. All these structural superiorities of $C_{16}C_4C_{16}Br_2$ over CTAB together with lower C_1 values than CTAB are responsible for its stronger interaction with XO at a given surfactant concentration and hence larger change in FI_{350} .

Intrinsic Fluorescence. The shift in the wavelength of emission maximum (λ_{max}^{295nm}), a parameter sensitive to the protein conformations, can be used to examine the conformational changes of protein during their interaction with surfactants.⁴⁴ In a hydrophobic environment, such as the interior of a folded protein, tryptophan emission occurs at shorter wavelength.⁴⁹ Therefore, shift of emission maximum from shorter to longer wavelengths upon protein unfolding would correspond to the exposure of tryptophan residues to an aqueous environment. The amino acid sequence of each subunit in bovine milk XO includes 10 tryptophan residues.¹² The change in the wavelength of emission maximum by excitation at 295 nm, λ_{max}^{295nm} , is illustrated in Figure 3 and

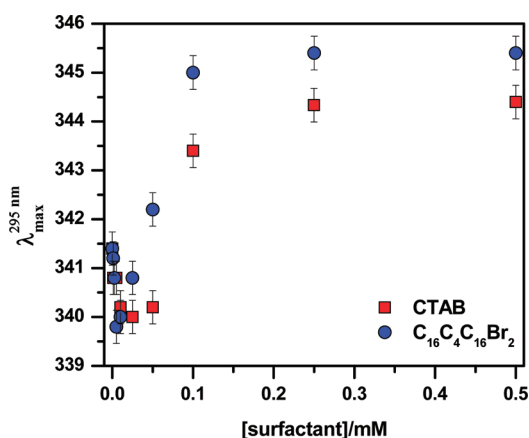


Figure 3. Variation of λ_{max}^{295nm} of 2 μ M XO solution with the concentration of CTAB and $C_{16}C_4C_{16}Br_2$ at pH 7.4 and 25 $^{\circ}$ C.

indicates that XO exhibits an initial small blue shift at very low surfactant concentrations followed by red shift at higher surfactant concentrations. The red shift increases with an increase in the concentration of the surfactant and then attains a constant value at higher surfactant concentrations. An increase in λ_{max}^{295nm} with an increase in surfactant concentration indicates a shift of fluorophores toward a more hydrophilic environment.⁴⁹ The constancy in λ_{max}^{295nm} , thereafter, point out no change in the environment around the tryptophan residues and suggests saturation of XO backbone by the micelles, in corroboration with the binding isotherms suggested for protein–surfactant interactions.⁵ Although the increasing trend of λ_{max}^{295nm} is similar in both CTAB and $C_{16}C_4C_{16}Br_2$, the red shift in λ_{max}^{295nm} is more when the XO interacts with $C_{16}C_4C_{16}Br_2$ (4.0 nm) than with CTAB (3.0 nm), a behavior

found similar to that with other proteins.^{26,28,31,47} At low surfactant concentrations, the little blue shift (1.5 nm) indicates more hydrophobicity perceived by the XO fluorophores than in its native state. At pH 7.4, XO appears as a polyion with considerable negative charges. Therefore, it is expected that the positively charged surfactant headgroups would bind preferably onto those negatively charged sites of XO where the alkyl chains of the surfactant also get stabilized through a hydrophobic effect to minimize the unfavorable contact with water. These bound alkyl chains of surfactant molecules acting as hydrophobic sites promote further binding of the surfactant molecules possibly enhancing the hydrophobicity of nearby fluorophores resulting in an initial blue shift. However, as the surfactant concentration is increased, the electrostatic repulsion between the micelle-like aggregates formed on XO exceeds the interactions supporting XO structure thereby unfolding XO and hence exposing the fluorophores to a polar aqueous environment to yield the red shift. Because of the doubly charged headgroup of $C_{16}C_4C_{16}Br_2$, its aggregates on XO are expected to experience more electrostatic repulsion thereby exposing the fluorophores to an aqueous environment to a greater extent than by the aggregates of CTAB.

Extrinsic Fluorescence. 1-Anilino-8-naphthalenesulphonate (ANS) is a widely used fluorescent hydrophobic probe for examining the nonpolar character of proteins.⁵⁰ The fluorescence of ANS bound to nonpolar sites of protein has been found equal to the fluorescence of an equal amount of ANS in a number of hydrophobic solvents.⁵⁰ There are two modes of ANS interaction with proteins.⁵¹ In the first mode, ANS has its anilinonaphthalene group located such that it is mostly or completely exposed to water quenching and therefore nonfluorescent. In the second mode, ANS has its anilinonaphthalene group located so that the hydrophobic patches of the protein protected it mostly or completely from water quenching and therefore becomes fluorescent. The fluorescence exhibited by the XO bound ANS is therefore attributed to the presence of the hydrophobic patches in the XO, and hence, the variation of the fluorescence intensity can be effectively used to monitor its accessibility to these hydrophobic patches. Bound ANS excites at 380 nm and emits maximally at 480 nm.

Figure 4 depicts the changes in fluorescence intensities at 480 nm with increasing concentrations of CTAB and $C_{16}C_4C_{16}Br_2$. Initially, XO shows a large increase in ANS binding, which slows down with increasing surfactant concentration and finally

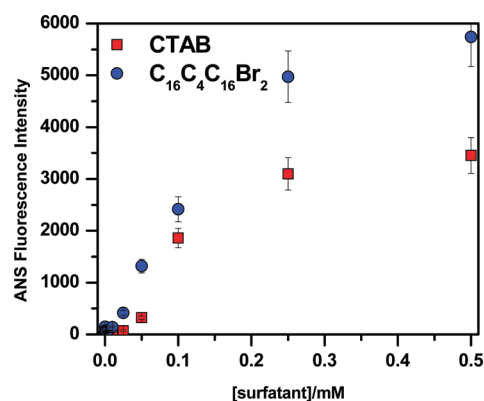


Figure 4. Variation of ANS fluorescence intensity at 480 nm in 2 μ M XO solution with the concentration of CTAB and $C_{16}C_4C_{16}Br_2$ at pH 7.4 and 25 $^{\circ}$ C.

assumes a constant value at higher surfactant concentrations. The increase in ANS binding, indicated by an increase in ANS fluorescence intensity, with surfactant concentration is associated with the increasing number of hydrophobic patches as the protein unfolds due to binding of the surfactant molecules. The saturation in ANS binding, thereafter, is consistent with the binding isotherms and suggests that the protein undergoes conformational changes only up to a particular surfactant concentration after which the protein backbone is saturated with micelles and further addition of the surfactant does not bring about any significant change.⁵ Because of the reasons mentioned in the above sections, considerable unfolding of XO by $C_{16}C_4C_{16}Br_2$ makes a greater number of hydrophobic patches of the XO accessible to ANS binding thereby enhancing the ANS fluorescence intensity more effectively (5719 A.U.) than CTAB (3432 A.U.).

UV–Visible Spectrophotometry. The absorption band at 277 nm is characteristic of aromatic residues (tryptophan) in XO.⁵² UV–visible absorption is sensitive to the environment around the absorbing moieties and is used to sense the change in protein conformation such as unfolding. The tryptophan absorption of a native protein can be greater or smaller than the absorption of free tryptophan in aqueous solution. Consequently, both increase and decrease in UV–visible absorption can occur upon protein unfolding.^{53–55} Figure 5 shows the

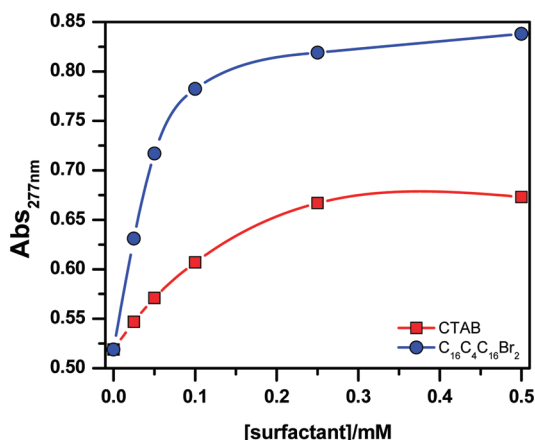
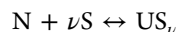


Figure 5. Variation of absorbance of 2 μ M XO solution at 277 nm with the concentration of CTAB and $C_{16}C_4C_{16}Br_2$ at pH 7.4 and 25 $^{\circ}C$.

change in absorbance of XO at 277 nm with the surfactant concentration indicating changes in the environment around the aromatic residues of XO on the interaction with the surfactants. Like λ_{max}^{295nm} and ANS fluorescence intensity, the UV–visible absorption first increases with an increase in the surfactant concentration and thereafter attains a constant value. The increase in UV–visible absorption also indicates the shift of aromatic residues toward the more polar aqueous environment due to unfolding of the XO, the increase being more pronounced in the presence of $C_{16}C_4C_{16}Br_2$ (0.838) than in CTAB (0.673). The constancy in the absorption intensity thereafter suggests that all the available binding sites have been occupied by the surfactants and/or micelle-like aggregates.

For the first approximation, thermodynamically, the transition between the native (N) and unfolded state with ν bound surfactant ligands (S) may be expressed by the equilibrium^{56,57}



where ν is the average number of surfactant molecules (S) bound to the unfolded complex (US_{ν}). The extent of unfolding measured by the fraction of unfolded molecules is given by^{56,57}

$$F_U = \frac{A_{277}^N - A_{277}}{A_{277}^N - A_{277}^U}$$

where A_{277} is the absorbance of XO at 277 nm at different surfactant concentrations, and A_{277}^N and A_{277}^U are the absorbances of the native and maximum unfolded XO at the same wavelength. A_{277}^U is taken as the absorbance of XO, which remains constant with the surfactant concentration.

The difference in the standard Gibbs energy between the native and unfolded conformations can be calculated as^{56,57}

$$\Delta G^{\circ} = -RT \ln \left[\frac{F_U}{1 - F_U} \right]$$

where R is the gas constant, and T is the absolute temperature. The variation of F_U as a function of surfactant concentration, shown in Figure 6, indicates that the fraction of XO, which is

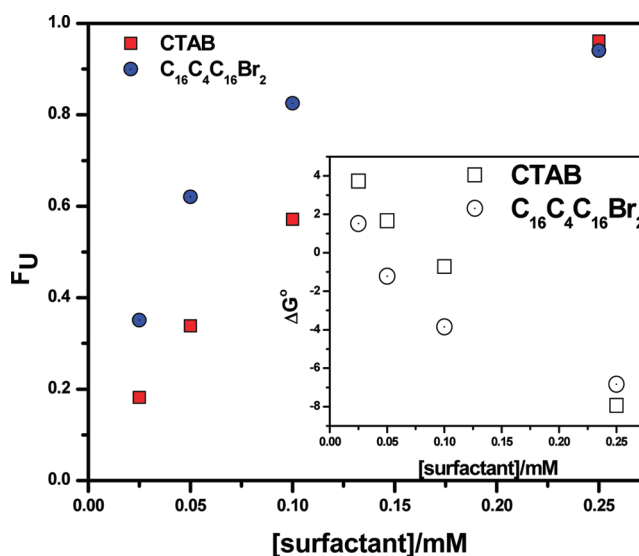


Figure 6. Variation of unfolded fraction, F_U , and difference in Gibbs free energy change, ΔG° (inset), of 2 μ M XO solution with the concentration of CTAB and $C_{16}C_4C_{16}Br_2$ at pH 7.4 and 25 $^{\circ}C$.

being unfolded by the surfactants, increases with an increase in the surfactant concentration and is greater in the presence of $C_{16}C_4C_{16}Br_2$ than CTAB. The above arguments are also supported by the variation of ΔG° with the surfactant concentration shown in the inset of the same figure. $C_{16}C_4C_{16}Br_2$, as expected due to its peculiar structural properties, is strongly driven to associate with XO and, together with its lower C_1 values, can unfold a larger fraction of XO than CTAB at a given surfactant concentration. Lower C_1 implies earlier aggregation of surfactant with XO and hence a large number of XO–surfactant aggregates at a given surfactant concentration.

Far-UV Circular Dichroism. Circular dichroism can be used to probe transitions in the secondary structure of the proteins. Figure 7 (left) shows far-UV CD spectra of native XO and XO in the presence of 0.1 mM CTAB and 0.1 mM $C_{16}C_4C_{16}Br_2$ at pH 7.4.

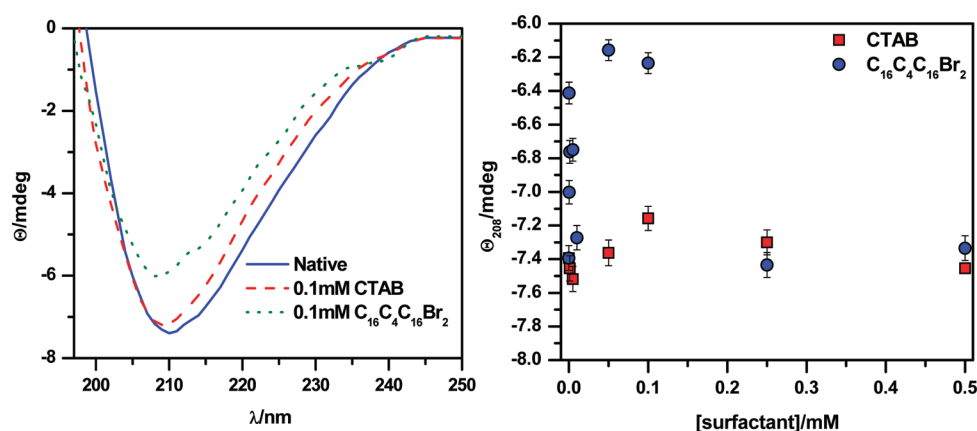


Figure 7. Far-UV CD spectra of native XO in the presence of 0.1 mM CTAB and 0.1 mM C₁₆C₄C₁₆Br₂ (left) and the effect of their concentration on the ellipticity at 208 nm of XO (right) at pH 7.4 and 25 °C.

Alterations in ellipticity at 208 nm (θ_{208}) are used to monitor the change in the secondary structure of XO as a function of CTAB and C₁₆C₄C₁₆Br₂. The effect of the surfactant concentration on the ellipticity of XO is also shown in Figure 7 (right). The negative value of ellipticity of XO decreases with an increase in surfactant concentration, indicating denaturation of XO, and then attains a maximum value. Afterward, the ellipticity begins to rise indicating the stabilization of the secondary structure of XO at higher surfactant concentrations. It is observed that C₁₆C₄C₁₆Br₂ decreases the negative value of ellipticity of XO by 1.44 millidegrees, while as its conventional homologue is able to decrease it only by 0.25 millidegrees, demonstrating an insignificant effect of the latter.

The denaturation of XO by the ionic surfactants may be attributed to the presence of adsorbed surfactant on the protein in the form of monomers and micelle-like aggregates, which break the hydrophobic interactions and facilitate the electrostatic repulsion thereby denaturing the XO. However, the stabilization of the XO structure by surfactants, particularly Gemini, at higher concentrations under elevated ionic strength indicates the role of micellar morphology, as all these conditions are usually associated with micellar growth. There are many factors, including the concentration,^{24,58–60} nature of surfactant,^{61,62} and presence of additives,^{63–69} which determine the shape of the micelles. At higher surfactant concentrations, the hydrodynamic radius of micelles increases appreciably due to micellar growth^{24,58–60} promoted by the presence of salts.^{63–69} Keeping in consideration the high ionic strength (60 mM phosphate buffer) of our system, the change in micellar morphology is expected at the higher surfactant concentrations. Gemini surfactants with a short spacer (≤ 5) have a much stronger tendency for micellar growth and aggregate into assemblies having the shape of vesicles and/or membrane fragments.^{61,62} The studies^{70–75} on the influence of the membrane/water interfacial region of bilayer upon protein conformations provide strong evidence that the partitioning of hydrophobic peptides into membrane-like environments is coupled to helix formation and hydrogen bonding. White and colleagues systematically studied the free energy changes associated with the transfer of unfolded peptides from water to octanol⁷⁶ and from water to the membrane interfacial region of 1-palmitoyl-2-oleoyl-*sn*-glycero-3-phosphocholine (POPC) bilayers⁷⁷ and suggested that the partitioning into the membrane interface of POPC is driven by the hydrophobic effect. According to them, the partitioning of an unfolded

peptide into the bilayer interface can drive folding of that peptide in the interface because of the increased favorable free energy associated with forming a hydrogen bond in the interfacial region compared to that in water. The property of surfactant aggregates to provide a membrane-like environment and the stabilization of protein structure by partitioning into the membrane/water interfacial region of surfactant assemblies, so far, seems to be the most plausible explanation for the structural stabilization of XO at higher surfactant concentration. Such a structural stabilization demands immobilization of XO into the interface, which might be associated with its compression/folding thereby decreasing the size of its complexes. This is confirmed by the decrease in FI₃₅₀ at higher concentration of the surfactants, as is clear from Figure 2. C₁₆C₄C₁₆Br₂ being structurally more close to lipids compared to CTAB, its aggregates are expected to provide an environment mimicking biological membranes, which might be the reason for the enhanced structural stabilization of XO by such aggregates.

This part of our study, that is, stabilization of XO structure by higher concentrations of surfactants, especially by Gemini, although satisfactorily correlated with the reported results on micellar morphology, the protein stabilization by membrane/water interface needs to be explored thoroughly with respect to nature and composition of the interface and the protein to be folded to reveal the exact mechanistic details involved.

Inhibition of XO Activity. The percentage inhibition (PI) of XO as a function of surfactant concentration, shown in Figure 8, indicates that the activity of XO is reduced in the presence of surfactants. In concurrence with the variation of CD strength as a function of surfactant concentration, inhibition of XO increases with an increase in the surfactant concentration, attains a maximum, and then drops again. The inhibition of XO activity may be ascribed to the loss in its secondary structure induced by the surfactants. PI of XO goes up to 17.69 and finally drops to 8.5 with increasing [CTAB], while, with increasing [C₁₆C₄C₁₆Br₂] after attaining a maximum at 25.26, PI of XO falls to 2.5. The gain in activity of XO at higher concentrations of the surfactants, especially C₁₆C₄C₁₆Br₂, may be attributed to the stabilization of XO structure by the membrane/water interface of surfactant aggregates as indicated by the CD results and supported by the aggregation data.

In agreement with an earlier report,⁷⁸ the formation of C₁ evidenced in tensiometry is missing in the spectroscopic

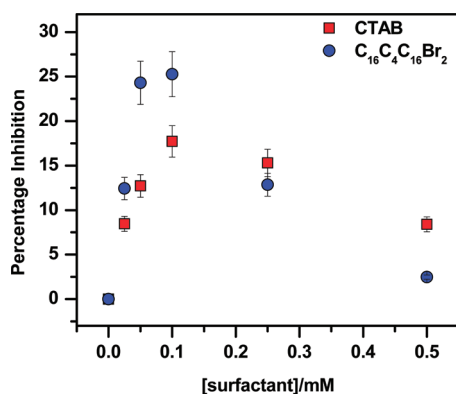


Figure 8. Variation of percentage inhibition of 2 μ M XO solution with the concentration of CTAB and $C_{16}C_4C_{16}Br_2$ at pH 7.4 and 25 $^{\circ}C$.

measurements. By means of the techniques employed in the present study, a molecular understanding of the variation of XO activity with surfactant concentration could not be made, which may be possible by employing more ingenious methods.

CONCLUSIONS

The results of the present study reveal the existence of interaction between the surfactants and XO. Rayleigh's scattering, tryptophan fluorescence, ANS binding, and spectrophotometric studies showed that the extent of unfolding of XO induced by $C_{16}C_4C_{16}Br_2$ is more than that by CTAB. CD results also confirmed that $C_{16}C_4C_{16}Br_2$ is more effective in destabilizing the secondary structure of XO and inhibiting its activity. However, there is regain in the activity of XO at higher concentrations of $C_{16}C_4C_{16}Br_2$ indicating that the partitioning of unfolded protein is driven by more favorable free energy change coupled with helix and hydrogen bond formation in the interfacial region than in bulk water. Before asserting any medical/biological implication of the present study, the interaction of the metabolically important enzyme XO with detergents needs to be explored further both in vitro as well as in vivo.

AUTHOR INFORMATION

Corresponding Author

*E-mail: aijaz_n5@yahoo.co.in (A.A.D.); gmrather2002@yahoo.com (G.M.R.).

Present Address

[§]Government Degree College for Women, Anantnag, Department of Higher Education, J&K, India.

Notes

The authors declare no competing financial interest.

ACKNOWLEDGMENTS

We are thankful to the Head Department of Chemistry, University of Kashmir, for providing the laboratory facilities and his constant encouragement and inspiration. M.A.M. (J.R.F.) acknowledges the financial support [File No.: 09/251(0021)/2008-EMR-I] from the Council of Scientific and Industrial Research, India.

REFERENCES

(1) Ananthapadmanabhan, K. P. In *Interactions of Surfactants with Polymers and Proteins*; Goddard, E. D., Ananthapadmanabhan, K. P., Eds.; CRC Press, Inc.: London, UK, 1993; Chapter 8.

- (2) Jones, M. N. *Chem. Soc. Rev.* **1992**, 21, 127–136.
- (3) Jones, M. N. In *Food Polymers, Gels and Colloids*; The Royal Society of Chemistry: Cambridge, UK, 1991; pp 65–80.
- (4) McClements, D. J. *Food Emulsions: Principles, Practice and Techniques*, 2nd ed.; CRC Press: Boca Raton, FL, 2004.
- (5) Few, A. V.; Ottewill, R. H.; Parreira, H. C. *Biochim. Biophys. Acta* **1955**, 18, 136–137.
- (6) Nozaki, Y.; Reynolds, J. A.; Tanford, C. J. *Biol. Chem.* **1974**, 249, 4452–4459.
- (7) Takeda, K.; Hachiya, K.; Moriyama, Y. *Interaction of Protein with Ionic Surfactants: Part 2*; Marcel Dekker: New York, 2002; p 2575.
- (8) Doeber, W.; Anker, S. D. *Heart* **2005**, 91, 707–709.
- (9) Berry, C. E.; Hare, J. M. J. *Physiol* **2004**, 555, 589–606.
- (10) Harrison, R. *Free Radical Biol. Med.* **2002**, 33, 774–797.
- (11) McCord, J. M. *N. Engl. J. Med.* **1985**, 312, 159–163.
- (12) Enroth, C.; Eger, B. T.; Okamoto, K.; Nishino, T.; Pai, E. *Proc. Natl. Acad. Sci. U.S.A.* **2000**, 97, 10723–10728.
- (13) Hille, R. *Chem. Rev.* **1996**, 96, 2757–2816.
- (14) Huber, R.; Hof, P.; Duarte, R. O.; Moura, J. G.; Moura, I.; Liu, M. Y.; LeGall, J. *Proc. Natl. Acad. Sci. U.S.A.* **1996**, 93, 8846–8851.
- (15) Doonan, C. J.; Stockert, A.; Hille, R.; George, G. N. *J. Am. Chem. Soc.* **2005**, 127, 4518–4522.
- (16) Lee, C.; Liu, X.; Zweier, J. L. *J. Biol. Chem.* **2000**, 275, 9369–9376.
- (17) Fernandes, A. S.; Gaspar, J.; Cabral, M. F.; Caneiras, C.; Guedes, R.; Rueff, J.; Castro, M.; et al. *J. Inorg. Biochem.* **2007**, 101, 849–858.
- (18) Sau, A. K.; Mondal, M. S.; Mitra, S. *Biochim. Biophys. Acta* **2001**, 1544, 89–95.
- (19) Mondal, M. S.; Mitra, S. *J. Inorg. Biochem.* **1996**, 62, 271–279.
- (20) Ghio, A. J.; Kennedy, T. P.; Stonehuerner, J.; Carter, J. D.; Skinner, K. A.; Parks, D. A.; Hoidal, J. R. *Am. J. Physiol. Lung Cell Mol. Physiol.* **2002**, 283, L563–L572.
- (21) Lovstad, R. A. *BioMetals* **2003**, 16, 435–439.
- (22) Zana, R.; Xia, J., Eds. *Gemini Surfactants*; Marcel Dekker: New York, 2003.
- (23) Zana, R. *Adv. Colloid Interface Sci.* **2002**, 97, 205–253.
- (24) Siddiqui, U. S.; Ghosh, G.; Kabir-ud-Din. *Langmuir* **2006**, 22, 9874–9878.
- (25) Wettig, S. D.; Verrall, R. E.; Foldvari, M. *Curr. Gene Ther.* **2008**, 8, 9–23.
- (26) Li, Y.; Wang, X.; Wang, Y. *J. Phys. Chem. B* **2006**, 110, 8499–8505.
- (27) Pi, Y.; Shang, Y.; Peng, C.; Liu, H.; Hu, Y.; Jiang, J. *Biopolymers* **2006**, 83, 243–249.
- (28) Wu, D.; Xu, G.; Feng, Y.; Li, Y. *Int. J. Biol. Macromol.* **2007**, 40, 345–350.
- (29) Wu, D.; Xu, G.; Sun, Y.; Zhang, H.; Mao, H.; Feng, Y. *Biomacromolecules* **2007**, 8, 708–712.
- (30) Gull, N.; Sen, P.; Khan, R. H.; Kabir-ud-Din. *J. Biochem.* **2009**, 145, 67–77.
- (31) Gull, N.; Sen, P.; Khan, R. H.; Kabir-ud-Din. *Langmuir* **2009**, 25, 11686–11691.
- (32) Kabir-ud-Din; Fatma, W.; Khan, Z. A.; Dar, A. A. *J. Phys. Chem. B* **2007**, 111, 8860–8867.
- (33) Massey, V.; Brumby, P.; Komai, H. *J. Biol. Chem.* **1969**, 244, 1682–1691.
- (34) Nguyen, M. T. T.; Awale, S.; Tezuka, Y.; Ueda, J.; Tran, Q. L.; Kadota, S. *Planta Med.* **2006**, 72, 46–51.
- (35) Moulik, S. P.; Ghosh, S. *J. Mol. Liq.* **1997**, 72, 145–161.
- (36) Ghosh, S.; Moulik, S. P. *J. Colloid Interface Sci.* **1998**, 208, 357–366.
- (37) Ghosh, S. *J. Colloid Interface Sci.* **2001**, 244, 128–138.
- (38) Chakraborty, T.; Ghosh, S.; Moulik, S. P. *J. Phys. Chem. B* **2005**, 109, 14813–14823.
- (39) van Voorst Vader, F. *Trans. Faraday Soc.* **1960**, 56, 1067–1077.
- (40) Kabir-ud-Din; Sheikh, M. S.; Dar, A. A. *J. Colloid Interface Sci.* **2009**, 333, 605–612.
- (41) Dar, A. A.; Rather, G. M.; Das, A. R. *J. Phys. Chem. B* **2007**, 111, 3122–3132.

- (42) Lu, R. C.; Cao, A. N.; Lai, L. H.; Zhu, B. Y.; Zhao, G. X.; Xiao, J. X. *Colloids Surf., B* **2005**, *41*, 139–143.
- (43) Miller, R.; Fainerman, V. B.; Makievski, A. V.; Kragel, J.; Grigoriev, D. O.; Kazakov, V. N.; Sinyachenko, O. V. *Adv. Colloid Interface Sci.* **2000**, *86*, 39–82.
- (44) Fainerman, V. B.; Zholob, S. A.; Leser, M. E.; Michel, M.; Miller, R. J. *Phys. Chem.* **2004**, *108*, 16780–16785.
- (45) Sturgeon, B.; Chen, E. Y. R.; Mason, R. P. *Anal. Chem.* **2003**, *75*, 5006–5011.
- (46) Xia, J.; Zhang, H.; Rigsbee, D. R.; Dubin, P. L.; Shaikh, T. *Macromolecules* **1993**, *26*, 2759–2766.
- (47) Mir, M. A.; Khan, J. M.; Dar, A. A.; Khan, R. H.; Rather, G. M. *Colloids Surf., B* **2010**, *77*, 54–59.
- (48) Zhao, X.; Shang, Y.; Liu, H.; Hu, Y. J. *Colloid Interface Sci.* **2007**, *314*, 478–483.
- (49) Deep, S.; Ahluwalia, J. C. *Phys. Chem. Chem. Phys.* **2001**, *3*, 4583–4591.
- (50) Stryer, L. *J. Mol. Biol.* **1965**, *13*, 482–495.
- (51) Matulis, D.; Baumann, C. G.; Bloomfield, V. A.; Lovrien, R. E. *Biopolymers* **1999**, *49*, 451–458.
- (52) Hadizadeh, M.; Keyhani, E.; Keyhani, J.; Khodadadi, C. *Acta Biochim. Biophys. Sin.* **2009**, *41*, 603–617.
- (53) Gaggelli, E.; Berti, F.; D'Amelio, N.; Gaggelli, N.; Valensin, G.; Bovalini, L.; Paffetti, A.; Trabalzini, L. *Environ. Health Perspect.* **2002**, *110*, 733–738.
- (54) Sun, C.; Yang, J.; Wu, X.; Huang, X.; Wang, F.; Liu, S. *Biophys. J.* **2005**, *88*, 3518–3524.
- (55) Schmid, F. X. Biological Macromolecules: UV-visible Spectrophotometry. In *Encyclopedia of Life Sciences*; Macmillan Publishers Ltd.: London, U.K., 2001.
- (56) Prieto, G.; Suarez, M. J.; Gonzalez-Perez, A.; Ruso, J. M.; Sarmiento, F. *Phys. Chem. Chem. Phys.* **2004**, *6*, 816–821.
- (57) Messina, P. V.; Prieto, G.; Ruso, J. M.; Sarmiento, F. J. *Phys. Chem. B* **2005**, *109*, 15566–15573.
- (58) Birdi, K. S. *Micellization, Solubilization and Microemulsion*; Mittal, K. L., Ed.; Plenum Press: New York, 1977.
- (59) Ekwall, P.; Mandell, L.; Solyom, P. J. *Colloid Interface Sci.* **1971**, *35*, 519–528.
- (60) Imae, T.; Kamiya, R.; Ikeda, S. J. *Colloid Interface Sci.* **1985**, *108*, 215–225.
- (61) Zana, R.; Talmon, Y. *Nature* **1993**, *362*, 228–230.
- (62) Danino, D.; Talmon, Y.; Zana, R. *Langmuir* **1995**, *11*, 1448–1456.
- (63) Kumar, S.; Aswal, V. K.; Singh, H. N.; Goyal, P. S.; Kabir-ud-Din. *Langmuir* **1994**, *10*, 4069–4072.
- (64) Kabir-ud-Din; Kumar, S.; Kirti; Goyal, P. S. *Langmuir* **1996**, *12*, 1490–1494.
- (65) Kabir-ud-Din; Bansal, D.; Kumar, S. *Langmuir* **1997**, *13*, 5071–5075.
- (66) Kumar, S.; Bansal, D.; Kabir-ud-Din. *Langmuir* **1999**, *15*, 4960–4965.
- (67) Kumar, S.; David, S. L.; Kabir-ud-Din. *J. Am. Oil Chem. Soc.* **1997**, *74*, 797–801.
- (68) Kumar, S.; David, S. L.; Aswal, V. K.; Goyal, P. S.; Kabir-ud-Din. *Langmuir* **1997**, *13*, 6461–6464.
- (69) Kumar, S.; Aswal, V. K.; Goyal, P. S.; Kabir-ud-Din. *J. Chem. Soc., Faraday Trans.* **1998**, *94*, 761–764.
- (70) White, S. H.; Wimley, W. C. *Annu. Rev. Biophys. Biomol. Struct.* **1999**, *28*, 319–365.
- (71) White, S. H.; Wimley, W. C. *Biochim. Biophys. Acta* **1998**, *1376*, 339–352.
- (72) Nozaki, Y.; Tanford, C. J. *Biol. Chem.* **1971**, *246*, 2211–2217.
- (73) Jacobs, R. E.; White, S. H. *Biochemistry* **1989**, *28*, 3421–3437.
- (74) Li, S. C.; Deber, C. M. *Nat. Struct. Biol.* **1994**, *1*, 368–373.
- (75) O'Neil, K. T.; DeGrado, W. F. *Science* **1990**, *250*, 646–651.
- (76) Wimley, W. C.; Creamer, T. P.; White, S. H. *Biochemistry* **1996**, *35*, 5109–5124.
- (77) Wimley, W. C.; White, S. H. *Nat. Struct. Biol.* **1996**, *3*, 842–848.
- (78) Chakraborty, T.; Chakraborty, I.; Moulik, S. P.; Ghosh, S. J. *Phys. Chem. B* **2007**, *111*, 2736–2746.